ASSESSMENT OF TWO-END DATA FAULT LOCATION ALGORITHMS FOR TRANSMISSION GRIDS

Eng. **Marian DRAGOMIR** PhD[1], Prof. Eng. **Marcel ISTRATE** PhD[2],
Eng. **Răzvan BENIUGĂ** PhD Stud.[2], Assist. Prof. Eng. **Dragoş MACHIDON**[2]

[1]CNTEE Transelectrica
[2]Technical University „Gh. Asachi"of Iaşi, Electrical Engineering Faculty, Power Engineering Department

REZUMAT. Defectele din reţelele electrice trebuie localizate rapid şi precis în vederea menţinerii stabilităţii reţelei şi a minimizării timpului de ieşire din funcţionare a liniei cu defect. Rezultate precise se pot obţine dacă se utilizează algoritmi de localizare a defectelor ce folosesc date de la ambele extremităţi ale liniei. Se prezintă câteva rezultate ce permit evaluarea algoritmilor propuşi în funcţie de erorile introduse. Rezultatele au fost obţinute cu ajutorul transpunerii în Matlab a unei reţele de 400 kV.

Cuvinte cheie: algoritmi de localizare cu date de la ambele extremitati; eroare de estimare.

ABSTRACT. Accurate results can be achieved if there are employed fault location algorithms which use data from both ends of the line. Some results regarding the fault location errors provided by three fault location algorithms are presented. The results were obtained by transposing into Matlab a simple 400 kV grid.

Keywords: two-end data fault location algorithm; error estimation.

1. INTRODUCTION

Transmission line faults have to be located quickly and accurately in order to repair the faulted section, restore power delivery and reduce outage time as much as possible.

Taking into account the components from the fault signal that are processed to estimate the fault location, the actual fault location algorithms can be divided in two main categories namely: those who process the power frequency components and those who process the high frequency components [1], [2].

The two-end data fault location algorithms employed in this study are those of Chen [6], Istrate [5] and Tziouvaras [4]. The first one processes the voltage and current synchrophasors from both ends of the line, while the second one processes only the unsynchronized voltages from both ends of the line and the third one processes only the unsynchronized currents from both ends of the line. For estimation of the fault location, the power frequency phasors of the voltage and current are estimated with an adaptive algorithm indicated by Rosolowsky *et al*. [3].

In modern power grids the trend is to implement Phasor Measurement Unit (PMU) which makes possible the communication between the remote ends of the power grids' lines. Forward, using these PMUs, it can be implemented the Wide Area System (WAS) for monitoring and eventually for protection of the power grid. In these conditions it is possible to use the measurements of the PMUs and thus to implement the two-end data fault location algorithms.

2. FAULT LOCATION

Phasor estimation algorithm

From the literature [3] is well known that the classic full-period Fourier algorithm provide good results in phasor estimation when the fault signal contains no exponentially decaying dc component. The presence of such dc components in the fault signal may raise stability issues in the outputs of the classic full-period Fourier algorithm, which are more obvious for the fault current. Taking in account this remark, in [3] is presented a phasor estimation algorithm which starts from the classic full-period Fourier algorithm and adaptively suppresses an exponentially decaying dc component.

The orthogonal components of the power frequency phasor computed with the phasor estimation algorithm are as:

$$X_R[n] = X_C[n] - \delta_c[n] \quad (1)$$

$$X_I[n] = X_S[n] - \delta_s[n] \quad (2)$$

where $X_C[n]$ and $X_S[n]$ are the orthogonal components computed with the classic full-period Fourier algorithm:

$$X_C[n] = \frac{2}{N}\sum_{i=1}^{N} x[n-i]\cos(\frac{i2\pi}{N}) \quad (3)$$

$$X_S[n] = -\frac{2}{N}\sum_{i=1}^{N} x[n-i]\sin(\frac{i2\pi}{N}) \quad (4)$$

and $\delta_c[n]$, $\delta_s[n]$ are the corrections functions:

$$\delta_c[n] = d_c[n]X_0[n],\ \delta_s[n] = d_s[n]X_0[n] \quad (5)$$

where $x[n]$ is a generic sample from the measured fault signal with $n = 1, 2,\ldots, M$ (M is the number of samples considered), N is the number of samples in a fundamental period, equal in this case with the number of samples in the data window of the full-period Fourier algorithm, and i is the i^{th} sample in the data window.

Regarding (5), $d_c[n]$ and $d_s[n]$ are obtained using the formulas:

$$d_c[n] = D\cos(\frac{2\pi}{N}n + \delta) \quad (6)$$

$$d_s[n] = D\sin(\frac{2\pi}{N}n + \delta) \quad (7)$$

Also from the measured fault signal $x[n]$ there is computed an exponentially decaying dc component:

$$X_0[n] = \frac{2}{N}\sum_{i=1}^{N} x[n-i] \quad (8)$$

Regarding (6), D and δ are computed as:

$$D = \frac{1-\exp\frac{-T_1}{N\tau}}{\sqrt{\left(\cos\frac{2\pi}{N}-\exp\frac{-T_1}{N\tau}\right)^2-\sin^2\frac{2\pi}{N}}} \quad (9)$$

$$\delta = \tan^{-1}\left(\frac{\sin\frac{2\pi}{N}}{\cos\frac{2\pi}{N}-\exp\frac{-T_1}{N\tau}}\right) \quad (10)$$

with $T1$ being the fundamental period of the power frequency. The term $r = \exp(-T1/N\tau)$ depends on the unknown value of the time constant τ of the exponentially decaying dc component and can be estimated from the measurements at each sample:

$$r = r[n] = \frac{X_0[n]}{X_0[n-1]} \quad (11)$$

Equation (11) was obtained taking into account (8) where $X_0[n]$ stands for a sum of N elements of geometric progression with multiplier r. For stabilizing the estimator (11) there may be defined apriori values for r as:

$$r_{\min} \le r \le r_{\min} \quad (12)$$

where *rmin* and *rmax* are fixed values in accordance with the minimum and maximum assumed values of the time constant τ of the exponentially dc component.

Fault location algorithms

First it is considered a simple two-machine grid which has the equivalent model as in figure 1.

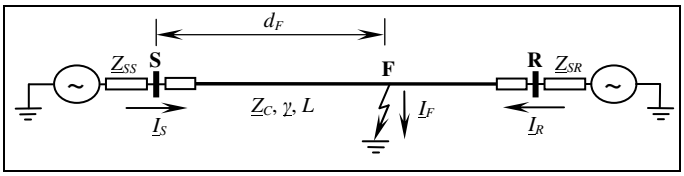

Fig. 1. One-line scheme of a faulty two-machine grid

In figure 1, with **S** and **R** denote the sending and the receiving ends of the line, $\underline{Z}_{SS}$, $\underline{Z}_{SR}$ are the equivalent sending end and receiving end sources impedances, $\underline{Z}_C$ and $\underline{\gamma}$ are the characteristic impedance and the propagation constant of the line which has the total length L; $\underline{\gamma} = \alpha + j\beta$, where α and β are the attenuation and phase constants; $\underline{I}_S$, $\underline{I}_R$ represent the sending end and the receiving end currents, $\underline{I}_F$ is the current at fault point **F** and d_F represent the distance to the fault measured from the sending end.

For a single phase to ground fault, the algorithm presented in [5] calculate the distance to the fault using the equation:

$$\tanh(\underline{\gamma}_1 d_F) = \underline{G} \quad (13)$$

where $\underline{G}$ is obtained from measurements as:

$$\underline{G} = \frac{1-\frac{(\underline{U}_R-\underline{U}_{R1})(\cosh\underline{\gamma}_1 L+\frac{\underline{Z}_{C1}}{\underline{Z}_{SR1}}\sinh\underline{\gamma}_1 L)}{\underline{U}_S-\underline{U}_{S1}}}{\frac{(\underline{U}_R-\underline{U}_{R1})(\sinh\underline{\gamma}_1 L+\frac{\underline{Z}_{C1}}{\underline{Z}_{SR1}}\cosh\underline{\gamma}_1 L)}{\underline{U}_S-\underline{U}_{S1}}-\frac{\underline{Z}_{C1}}{\underline{Z}_{SS1}}} \quad (14)$$

Regarding (13), after the calculations are made there is obtained a system of two equations as:

$$\begin{cases}\dfrac{1-\tan^2\beta_1 d_F}{1+(\tanh\alpha_1 d_F\tan\beta_1 d_F)^2}\tanh\alpha_1 d_F = W\\ \dfrac{1-\tanh^2\alpha_1 d_F}{1+(\tanh\alpha_1 d_F\tan\beta_1 d_F)^2}\tan\beta_1 d_F = Y\end{cases} \quad (15)$$

where d_F is calculated using a numerical solution and W, Y are the real and respectively the imaginary parts of $\underline{G}$. Regarding equations (13)÷(15), the subscript "1" denote the positive sequence, while in (14) $\underline{U}_S$, $\underline{U}_R$ represent the voltages on the faulted phase and $\underline{U}_{S1}$, $\underline{U}_{R1}$ represent the posivite sequence voltages at end **S** and end **R** of the considered line.

Another fault location algorithm is presented in [6], where the distance to the fault is calculated as:

$$d_F = L - \frac{\ln\dfrac{\underline{A}-\underline{C}}{\underline{E}-\underline{B}}}{2\underline{\gamma}_1} \tag{16}$$

where $\underline{A}$, $\underline{B}$, $\underline{C}$ and $\underline{E}$ are computed as:

$$\underline{A} = \frac{1}{2}(\underline{U}_{R1} + \underline{Z}_{C1}\underline{I}_{R1}) \tag{17}$$

$$\underline{B} = \frac{1}{2}(\underline{U}_{R1} - \underline{Z}_{C1}\underline{I}_{R1}) \tag{18}$$

$$\underline{C} = \frac{1}{2}(\underline{U}_{S1} + \underline{Z}_{C1}\underline{I}_{S1})\exp(\underline{\gamma}_1 L) \tag{19}$$

$$\underline{E} = \frac{1}{2}(\underline{U}_{S1} - \underline{Z}_{C1}\underline{I}_{S1})\exp(-\underline{\gamma}_1 L) \tag{20}$$

Algorithms presented in [5], [6] use the positive sequence quantities in the fault regime. Another approach is to use the negative sequence quantities as is shown in [4]. Considering the same grid depicted in figure. 1, the negative sequence scheme is:

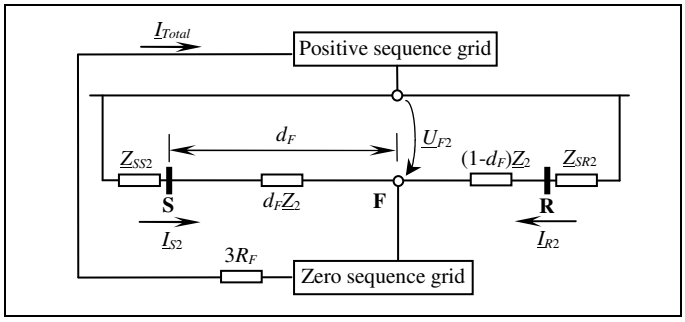

Fig. 2. The negative sequence scheme for a single phased fault

where the subscript "2" denote the negative sequence and R_F represents the fault resistance; $\underline{Z}_2$ represent the negative sequence specific impedance of the line.

The particularity of the negative sequence grid lies in the fact that the negative sequence voltage at the fault point is the same when viewed from all ends of the line:

End **S**: $$\underline{U}_{F2} = -\underline{I}_{S2}(\underline{Z}_{SS2} + d_F\underline{Z}_2) \tag{21}$$

End **R**: $$\underline{U}_{F2} = -\underline{I}_{R2}[\underline{Z}_{SR2} + (1-d_F)\underline{Z}_2] \tag{22}$$

Eliminating $\underline{U}_{F2}$, it is obtained:

$$\frac{\underline{I}_{S2}}{\underline{I}_{R2}} = \frac{\underline{Z}_{SR2} + (1-d_F)\underline{Z}_2}{\underline{Z}_{SS2} + d_F\underline{Z}_2} \tag{23}$$

where the only unknown is d_F.

3. SIMULATION RESULTS

In order to obtain the simulated faulty voltages and currents, the authors have modelled in Matlab a 400 kV transmission grid which has the nominal frequency fixed at 50 Hz. Also in Matlab there were imagined phasor estimation and fault location modules that take into account the equations used by each presented algorithm, as in figure 3.

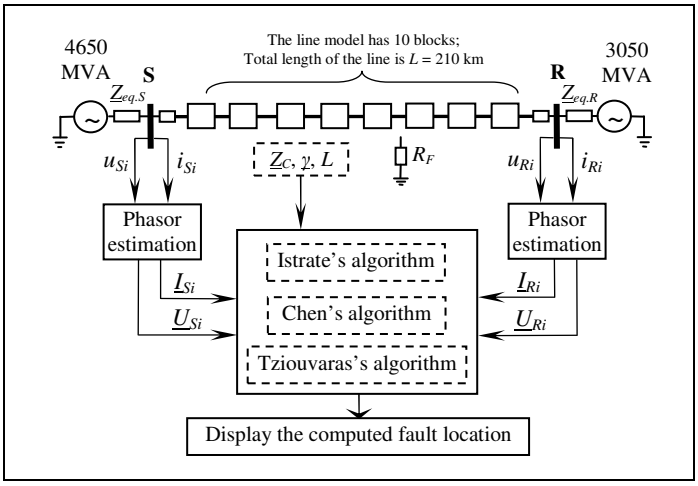

Fig. 3. The block-diagram of the fault locator

Regarding figure 3, the following notations were made: $\underline{Z}_{eq.S}$, $\underline{Z}_{eq.R}$ represent the equivalent sources impedances; the shortcircuit power of the source connected at end **S** is 4650 MVA and of the source connected at end **R** is 3050 MVA; u_{Si}, i_{Si}, u_{Ri}, i_{Ri} are the sampled voltages and currents obtained at end **S** and respectively **R** and $\underline{U}_{Si}$, $\underline{I}_{Si}$, $\underline{U}_{Ri}$, $\underline{I}_{Ri}$ are the associated phasors obtained with the phasor estimation module; in the fault location blocks are implemented the presented fault location algorithms and to compute the distance to the fault there are used, in addition, the line parameters; the transmission line is modeled by 10 blocks, each one corresponding to a 21 km line segment. The sequence parameters of the modeled transmission line are shown in table 1, where R is the resistance of the line, X is the reactance of the line, all in Ω/km and B is the susceptance of the line in S/km.

Table 1

Sequence parameters of the line

Seq. param.	R [Ω/km]	X [Ω/km]	B [S/km]
Pos. / Neg.	0,038	0,331	$3{,}4\cdot10^{-6}$
Zero	0,180	1,131	$2{,}3\cdot10^{-6}$

The simulation results presented in table 2 were obtained considering many single-phased faults along the modeled transmission line. In all cases, the fault's resistance R_F is considered 5 Ω, while the fault inception angle is considered π/2 rad.

The faults were simulated from ten to ten percent from total line's length, measured from end **S**. The computed fault locations are presented in two forms: in

[km] and [%] from total length of the line measured from end **S** of the line.

Table 2

Simulation results

Real fault location		Chen		Istrate		Tziouvaras	
[km]	[%]	[km]	[%]	[km]	[%]	[km]	[%]
21	10	27,88	13,28	27,78	13,23	28,47	13,56
42	20	46,242	22,02	48,11	22,91	47,14	22,45
63	30	65,751	31,31	65,79	31,33	66,27	31,56
84	40	86,163	41,03	86,66	41,27	86,81	41,34
105	50	106,722	50,82	107,60	51,24	107,70	51,29
126	60	127,785	60,85	128,35	61,12	128,75	61,31
147	70	148,911	70,91	149,24	71,07	149,96	71,41
168	80	170,268	81,08	170,12	81,01	171,19	81,52
189	90	191,604	91,24	190,97	90,94	192,12	91,49
210	100	212,94	101,4	211,91	100,91	213,69	101,76

From table 2 it can be observed that for Istrate's algorithm the estimations are continuously improved with the increase of the distance between the end of the line and the location of the fault. In the other hand, for Chen's and Tziouvaras' algorithms the estimations of the fault location are precise for distances between 30% ÷ 80% from total length of the line measured from end **S**. For all of the presented fault location algorithms it can be observed that the estimations are unprecise for short distances between the location of the fault and the end of the line.

4. CONCLUSIONS

In this paper there were presented some simulation results regarding the estimation accuracy of three fault location algorithms. In order to obtain the simulated faulty voltages and currents the authors modeled and then transposed into Matlab a simple high voltage grid as well as the fault location blocks. The fault location algorithms have in common the phasor estimation module presented in [3]. To compute the fault location, the algorithms of Istrate and Chen use the positive sequence quantities of the faulted grid, while the Tziuovaras' algorithm uses the negative sequence ones.

The results were obtained taking as parameter the location of the fault along the line when single phased faults were simulated.

The estimations provided by the above mentioned algorithms are unprecise when the fault takes place near the line's end, but they are highly impoved with the increase of the distance between the line's end and the location of the fault. In the case of Istrate's algorithm it is observed a continuous decrease of the fault location error with the increase of the distance measured from the location of fault and the line's end. In the case of the algorithms of Chen and Tziouvaras, the fault location errors are minimal when the fault takes place in the middle area of the faulted line.

BIBLIOGRAPHY

[1] *IEEE Guide for Determining Fault Location on AC Transmission and Distribution Lines*. IEEE Standard *C37.114*, 2005.

[2] **Saha M.M., Izykowski J., Rosolowsky E.,** *Fault Location on Power Networks*. Springer-Verlag, London, 2010.

[3] **Rosolowski E., Izykowski J., Kasztenny B**., *Adaptive Measuring Algorithm Suppressinga Decaying DC Component for Digital Protective Relays*. Electric Power Syst. Res., 60, *2*, 99-105 (2001).

[4] **Tziouvaras D.A., Roberts J.B., Benmouyal G**., *New Multi-Ended Fault Location Design for Two or Three-Terminal Lines*. IEE 7th Internat. Conf. on Develop. in Power Syst. Prot., Amsterdam, 2001, 395–398.

[5] **Istrate M., Miron A., Istrate C., Guşă M., Machidon D**., *Single-Phased Fault Location on Transmission Lines Using Unsynchronized Voltages*. Adv. in Electr. Comp. Engng., 9, *3*, 51-56 (2009).

[6] **Chen C.S., Liu C.W.**, *Fast and Accurate Fault Detection/Location Algorithms for Double-Circuit/Three-Terminal Lines Using Phasor Measurements Units*. J. of the Chinese Inst. of Eng., 26, *3*, 289-299 (2003).